ISSN 0015-4628, Fluid Dynamics, 2007, Vol. 42, No. 1, pp. 1–11. © Pleiades Publishing, Ltd., 2007.
Original Russian Text © S.V. Guvernyuk, G.Ya. Dynnikova, 2007, published in Izvestiya Rossiiskoi Akademii Nauk, Mekhanika Zhidkosti i Gaza, 2007, Vol. 42, No. 1, pp. 3–14.

Modeling the Flow Past an Oscillating Airfoil by the Method of Viscous Vortex Domains

S. V. Guvernyuk and G. Ya. Dynnikova

Received May 10, 2006

Abstract—The Lagrangian vortex method for solving the Navier–Stokes equations is applied for numerically modeling the unsteady flow past a wing airfoil executing angular oscillations in a viscous incompressible flow. Formulas relating the unsteady forces on the airfoil and the vorticity field are derived. The calculated results are compared with the experimental data for the NACA-0012 airfoil executing harmonic oscillations in an air flow at the Reynolds number $\mathrm{Re} = 4.4 \times 10^4$.

DOI: 10.1134/S0015462807010012

Keywords: viscous flows, unsteady flows, oscillating airfoil, Lagrangian vortex method.

The phenomenon of a sharp increase in the lift during the unsteady motion of an oscillating airfoil presents a topical problem of both engineering and fundamental importance. It can lead to additional variable loads on the lifting surfaces of maneuvering aircraft, the rotating blades of helicopters and compressors, and the flapping wings of birds or mechanical devices. At fairly high oscillation amplitudes and frequencies the stage of decrease of the angle of attack is accompanied by the generation of an intense vortex on the leeward side of the airfoil [1]. For a while, this vortex leads to a considerable increase in the lift and is then carried away into the wake. To understand and control the process, adequate numerical modeling of unsteady separated flows is necessary. Direct numerical simulation (solution of the time-dependent three-dimensional Navier–Stokes equations) could be such a method. However, this approach requires very large computational resources.

Though conventional engineering methods of numerical analysis based on the solution of the Reynolds equations can provide—given an appropriate choice of the turbulence model—results in agreement with experiment, the need to make this choice reduces the value of the method as far as its prediction possibilities are concerned. In particular, certain details of the time-dependent process required for the development of controls may turn out to be suppressed. The same can be said about widespread vortex methods based on the solution of the Euler equations (discrete vortex method, etc.), since their use involves the need to preassign separation points apriori or make additional assumptions concerning the body boundary-layer structure.

In this study, we shall attempt to model the unsteady flow past an oscillating airfoil using the viscous vortex domain method [2, 3] which is a numerical method for solving the two-dimensional Navier–Stokes equations in Lagrangian coordinates based on the notion of "diffusion velocity" [4, 5]. Moreover, the method used is refined and supplemented and formulas for calculating the unsteady stresses on the surface of a body in a viscous flow in terms of the vorticity distribution in the ambient space are derived.

1. FORMULATION OF THE PROBLEM

We will consider the time-dependent two-dimensional motion of a wing airfoil in an unbounded space filled with a viscous incompressible fluid, initially at rest. The fluid flow is governed by the Navier–Stokes and continuity equations

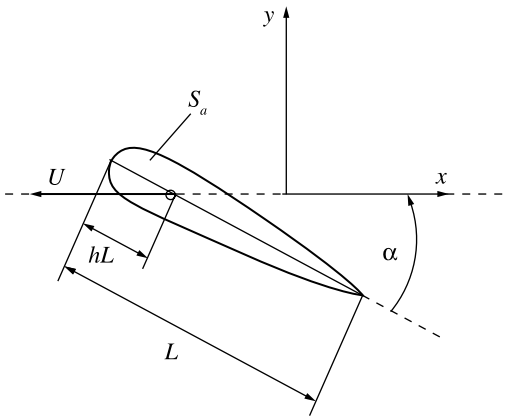

Fig. 1. Schematics of the wing airfoil motion.

$$\frac{\partial \mathbf{V}}{\partial t} - \mathbf{V}\times\boldsymbol{\Omega} = -\boldsymbol{\nabla}\left(\frac{p}{\rho} + \frac{V^2}{2}\right) + \nu\Delta\mathbf{V},$$
$$\boldsymbol{\nabla}\cdot\mathbf{V} = 0, \qquad \boldsymbol{\Omega} = \operatorname{curl}\mathbf{V}. \tag{1.1}$$

In the absolute Cartesian coordinate system $x,\ y$ the airfoil motion is governed by the law

$$\frac{dx_0}{dt} = \begin{cases} 0, & t \le 0 \\ -U, & t > 0, \end{cases} \qquad \frac{dy_0}{dt} = 0,$$

$$\alpha = \begin{cases} \alpha_0 - \alpha_1, & t \le 0 \\ \alpha_0 - \alpha_1\cos(2\pi f t), & t > 0. \end{cases}$$

Here, x_0 and y_0 are the Lagrangian coordinates of the O axis about which the airfoil S_a executes angular oscillations, t is time, α is the current angle between the chord and the x axis, U is the translational component of the wing velocity, α_0 is the mean angle of attack, α_1 is the amplitude of the angular oscillations about the mean value α_0, f is the circular oscillation frequency, L is the airfoil chord length, h is the relative distance from the leading edge to the oscillation axis, and C is a closed contour representing the airfoil S_a boundary (Fig. 1). In the two-dimensional motion under consideration the velocity vector $\mathbf{V}$ is parallel and the vorticity vector $\boldsymbol{\Omega}$ perpendicular to the $x,\ y$ plane. The pressure p is defined correct to an arbitrary constant (we will assume that $p = 0$ at infinity), while the density ρ and the kinematic viscosity ν are everywhere constant.

The initial conditions correspond to the state of rest throughout the entire $x,\ y$ space. The no-slip condition $\mathbf{V} = \mathbf{V}_C$ is imposed on the contour C, while at infinity the disturbances of all the functions vanish. The problem involves five dimensionless parameters

$$\alpha_0,\ \alpha_1,\ h,\ k = \pi L f/U, \qquad \mathrm{Re} = LU/\nu.$$

In what follows, we will use dimensionless variables scaling the linear dimensions and velocities on L and U, respectively, time on L/U, and the pressure and the other stresses on ρU^2.

From Eq. (1.1) there follows the vorticity transport equation [6]

$$\frac{\partial \boldsymbol{\Omega}}{\partial t} = \operatorname{curl}\left(\mathbf{V}\times\boldsymbol{\Omega} + \frac{1}{\mathrm{Re}}\Delta\mathbf{V}\right),$$

which, in accordance with [4, 5], can be written, using the definition of the diffusion velocity $\mathbf{V}_d$, in the form:

$$\frac{\partial \mathbf{\Omega}}{\partial t} = \mathrm{curl}((\mathbf{V} + \mathbf{V}_d) \times \mathbf{\Omega}), \qquad \mathbf{V}_d = -\frac{1}{\mathrm{Re}} \frac{\nabla \Omega}{\Omega}, \tag{1.2}$$

where Ω is the unique nonzero component of the vector $\mathbf{\Omega}$.

In an ideal fluid flow the circulation remains constant on "liquid" contours moving at the velocity $\mathbf{V}$ of the fluid (Helmholtz theorem); however, in a viscous flow this is usually not the case. Nevertheless, from Eq. (1.2) it follows that, if the viscous flow remains plane-parallel, then there are contours that possess the analogous property of circulation conservation in the process of motion, that is, the circulation remains constant on contours all of whose points move at the velocity $\mathbf{V} + \mathbf{V}_d$.

From Eqs. (1.1) and (1.2) we can also derive the following expression for the pressure:

$$\nabla p = \mathbf{V}_d \times \mathbf{\Omega} - \frac{d\mathbf{V}}{dt}. \tag{1.3}$$

The main problem consists in determining the unsteady vorticity field in the two-dimensional space S surrounding the airfoil S_a. The velocity field can be reconstructed from the vorticity field using known integral representations [6, 7], while the corresponding expressions for the pressure and viscous stresses on the body are derived below (Section 4).

In the comoving coordinate system x_a, y_a ($x_a = x + Ut$, $y_a = y$) fitted to the oscillation axis O (Fig. 1) we have a reverse motion, in which the fluid moves, while the wing executes purely angular oscillations in the fluid flow. Starting from a certain moment after oscillation onset, the flow past the airfoil tends to become quasi-periodic, like the analogous wind-tunnel flow, which makes it possible to draw corresponding comparisons with the experimental data.

2. METHOD OF NUMERICAL SOLUTION

The general scheme of the computational algorithm of the viscous vortex domain method is as follows. The domain S_a inside the airfoil is modeled by a fluid moving together with the airfoil as a rigid body, that is, with vorticity equal to 2ω, where ω is the angular velocity of the airfoil. For modeling the vorticity generation by the surface of the body in the viscous flow, in each time step a discrete set of vortex domains with circulations ensuring the fulfillment of the impermeability condition on the body contour is introduced near the surface. Then these newborn vortex domains move as Lagrangian particles on the velocity $\mathbf{V} + \mathbf{V}_d$, while the additional vorticity on the contour remains equal to zero; thanks to this, there is no velocity jump on the body surface and the no-slip boundary condition is automatically fulfilled. An analogous approach was used in the diffusion velocity method [4]; however, the viscous vortex domain method is free of certain significant shortcomings inherent in method [4]. In particular, a way of calculating the diffusion velocity $\mathbf{V}_d$ is developed such that, as distinct from [4], it ensures the correct determination of this velocity near the body surface. The problems associated with the approximation of the vorticity field $\mathbf{\Omega}$ by a sum of Gaussian distributions with a fixed radius, adopted in [4], are also overcome.

In Lagrangian methods, the calculation of the vorticity field gradient entering into formula (1.2) for the diffusion velocity $\mathbf{V}_d$ presents a very complicated problem. Here, we use an integral representation [3] based on the fact that any smooth scalar function $\Omega(\mathbf{r})$ given in a plane can be expressed in the form:

$$\Omega(\mathbf{R}) = \lim_{\varepsilon \to 0} \frac{1}{I} \int_S \Omega(\mathbf{r}) e^{-\xi}\, d\mathbf{r}', \qquad I = \int_S e^{-\xi}\, d\mathbf{r}'$$
$$\mathbf{r}' = \mathbf{r} - \mathbf{R}, \qquad d\mathbf{r}' = dx'dy', \qquad \boldsymbol{\xi} = \frac{\mathbf{r}'}{\varepsilon}. \tag{2.1}$$

In fact, substituting the expansion of the function

$$\Omega(\mathbf{r}) = \Omega(\mathbf{R}) + \mathbf{r}' \nabla \Omega(\mathbf{R}) + O(r'^2)$$

under the integral sign in Eq. (2.1), we obtain

$$\frac{1}{I}\int_S \Omega(\mathbf{R})e^{-\xi}\,d\mathbf{r}' = \Omega(\mathbf{R})$$
$$\frac{1}{I}\int_S (\mathbf{r}'\nabla\Omega(\mathbf{R}))e^{-\xi}\,d\mathbf{r}' = \varepsilon\nabla\Omega(\mathbf{R})\frac{1}{I}\int_S \boldsymbol{\xi}e^{-\xi}\,d\mathbf{r}'. \tag{2.2}$$

The integral ratio on the right-hand side of Eq. (2.2) is bounded (moreover, it can be shown that at points $\mathbf{R}$ which do not lie on the contour it vanishes as $\varepsilon \to 0$); from this there follows Eq. (2.1).

On the basis of Eq. (2.1) we can write

$$\frac{\nabla\Omega(\mathbf{R})}{\Omega} \approx \int_S \Omega(\mathbf{r})\frac{\boldsymbol{\xi}}{r'}e^{-\xi}\,d\mathbf{r}'\left[\int_S \Omega(\mathbf{r})e^{-\xi}\,d\mathbf{r}'\right]^{-1} - \frac{1}{I}\int_S \frac{\boldsymbol{\xi}}{r'}e^{-\xi}\,d\mathbf{r}'. \tag{2.3}$$

On the right-hand side of expression (2.3) the second term is independent of the vorticity distribution; it depends only on the geometry of the flow region S and the position of point $\mathbf{R}$. We will designate it by $-\mathbf{W}(\mathbf{R})$. The integral in the numerator of $\mathbf{W}$ can be transformed into a contour integral as follows:

$$\int_S \frac{\mathbf{r}'}{\varepsilon r'}e^{-\xi}\,d\mathbf{r}' = -\int_S \nabla e^{-\xi}\,d\mathbf{r}' = \oint_C \mathbf{n}e^{-\xi}\,dl. \tag{2.4}$$

Here, $\mathbf{n}$ is the outward normal to the surface contour and l is the distance measured along the surface.

In the case in which the distance from an internal point of the flow region to the region S boundary is much greater than ε, the integral I in the denominator of the expression for $\mathbf{W}$ calculated for this point is equal to $2\pi\varepsilon^2$, while for a point lying on a boundary interval whose length is much greater than ε it is equal to $\pi\varepsilon^2$. This can easily be verified, since the corresponding quadrature can be calculated analytically in polar coordinates. For an arbitrary point of region S this integral can be transformed into a contour integral. For this purpose, we will use the relation

$$e^{-\xi} = -\varepsilon\nabla\left(\frac{\mathbf{r}'(r' + \varepsilon)}{r'^2}e^{-\xi}\right)$$

which can be verified by differentiating the right side. Then, using the Stokes theorem, we obtain

$$\int_S e^{-\xi}\,d\mathbf{r}' = -\int_S \varepsilon\boldsymbol{\nabla}\left(\frac{\mathbf{r}'(r' + \varepsilon)}{r'^2}e^{-\xi}\right)d\mathbf{r}'$$
$$= -\oint_C \varepsilon\mathbf{n}\left(\frac{\mathbf{r}'(r' + \varepsilon)}{r'^2}e^{-\xi}\right)dl - \oint_{C_\delta} \varepsilon\mathbf{n}\left(\frac{\mathbf{r}'(r' + \varepsilon)}{r'^2}e^{-\xi}\right)dl,$$

where the contour C_δ is a circle of infinitely small radius drawn around the point $\mathbf{r}' = 0$. The integral over this contour is equal to $-2\pi\varepsilon^2$; therefore, we have

$$\int_S e^{-\xi}\,d\mathbf{r}' = 2\pi\varepsilon^2 - \oint_C \varepsilon\mathbf{n}\left(\frac{\mathbf{r}'(r' + \varepsilon)}{r'^2}e^{-\xi}\right)dl. \tag{2.5}$$

Finally, using Eqs. (2.3) to (2.5) and replacing the integrals by sums over discrete domains S_i with known circulations Γ_i we can write a discrete approximation for the diffusion velocity $\mathbf{V}_d$ in Eq. (1.2)

$$\begin{gathered}\mathbf{V}_{d_i} \approx \frac{1}{\mathrm{Re}}\sum_j \frac{\Gamma_j \mathbf{r}_{ij}}{\varepsilon r_{ij}} \exp\left(\frac{-r_{ij}}{\varepsilon}\right)\left(\sum_j \Gamma_j \exp\left(\frac{-r_{ij}}{\varepsilon}\right)\right)^{-1} + \mathbf{W}_i,\\ \mathbf{W}_i = \sum_k \mathbf{w}_{ik}, \qquad \mathbf{w}_{ik} = \frac{1}{\mathrm{Re}}\frac{\mathbf{n}_k d_k}{s_i}\exp\left(\frac{-r_{ik}}{\varepsilon}\right),\\ s_i = 2\pi\varepsilon_i^2 + \sum_k \varepsilon(\mathbf{n}_k \mathbf{r}_{ik})\frac{r_{ik}+\varepsilon}{r_{ik}^2}\exp\left(\frac{-r_{ik}}{\varepsilon}\right),\\ \mathbf{r}_{ij} = \mathbf{r}_i - \mathbf{r}_j; \qquad \mathbf{r}_{ik} = \mathbf{r}_i - \frac{\mathbf{r}_k + \mathbf{r}_{k+1}}{2}; \qquad d_k = |\mathbf{r}_{k+1} - \mathbf{r}_k|.\end{gathered} \tag{2.6}$$

Here, summation over the index k means summation over the contour intervals and $\mathbf{r}_k$ are gridpoint coordinates. If the accuracy of calculation of the integrals (2.4) and (2.5) written in the form of finite sums needs to be increased, then the contour intervals should be divided into smaller parts.

As can be seen from expression (2.6), the contribution of domain j to the diffusion velocity at point i is a vector directed along the line connecting points i and j; it is repulsive for circulations of the same sign and attractive if they are opposite in sign. The contribution decays exponentially with the distance between the points.

The vector $\mathbf{W}_i$ is the sum of the vectors $\mathbf{w}_{ik}$ representing the contributions of the contour intervals to the diffusion velocity at point i.

The contribution of each interval is directed normal to the interval and is repulsive irrespective of the circulation sign. If the distance to the wall is much greater than ε, then the contribution of this interval vanishes.

Going over from an integral to a finite sum produces an error due to the fact that inside the domain the integrand is not constant. In order for the function $\exp(-|\mathbf{r} - \mathbf{r}_i|/\varepsilon)$ entering into the integrand to vary weakly within the domain, the value of ε must be much greater than the linear dimensions of the domain. On the other hand, with increase in ε the error of representation (2.3) also increases. Moreover, the function Ω itself must be weakly variable inside the domain. Under the condition of existence of a smooth solution, the error can be made arbitrarily small in the limit of an infinitely divided domain.

In the course of the numerical simulation, we will keep track of a finite number of Lagrangian points, assuming that each point lies within a domain with a time-independent circulation. In the process of motion the contour boundaries may be deformed; as a result, the domain may turn out to be considerably extended. In this case, the contours can be mentally reclosed in such a way that the circulation of the domain surrounding each point remains invariable, while its form becomes more compact. This can be done, for example, by searching through pairs of neighboring domains and so replacing the extended boundary between them by a shorter boundary that the circulation of each domain remains the same. Though this reasoning is not rigorous, observation of the nature of the distribution of the selected points suggests that this is possible. Since the positions of the domain boundaries do not enter into the formulas, the particular choice is of no importance. All that matters is that the entire vorticity is distributed over a finite number of domains, while the information on each domain is carried by the corresponding Lagrangian point.

For calculating the diffusion velocity from formula (2.6), the value of the parameter ε for each point is chosen on the basis of the following rule. For point i the distance to the nearest point j (or to several nearest points) is determined by searching through all the points; then ε_i is taken to be equal to this distance multiplied by a certain margin c ($c > 1$). In formula (2.6), when summing over j, a j-independent value $\varepsilon = \varepsilon_i$ is used. Thus, the value of ε is chosen from the local characteristics of the control point distribution. In this case, a situation can arise, in which in summing over all the domains in formula (2.6) the value of ε is insufficiently large, as compared with the dimensions of distant domains. However, since the domain

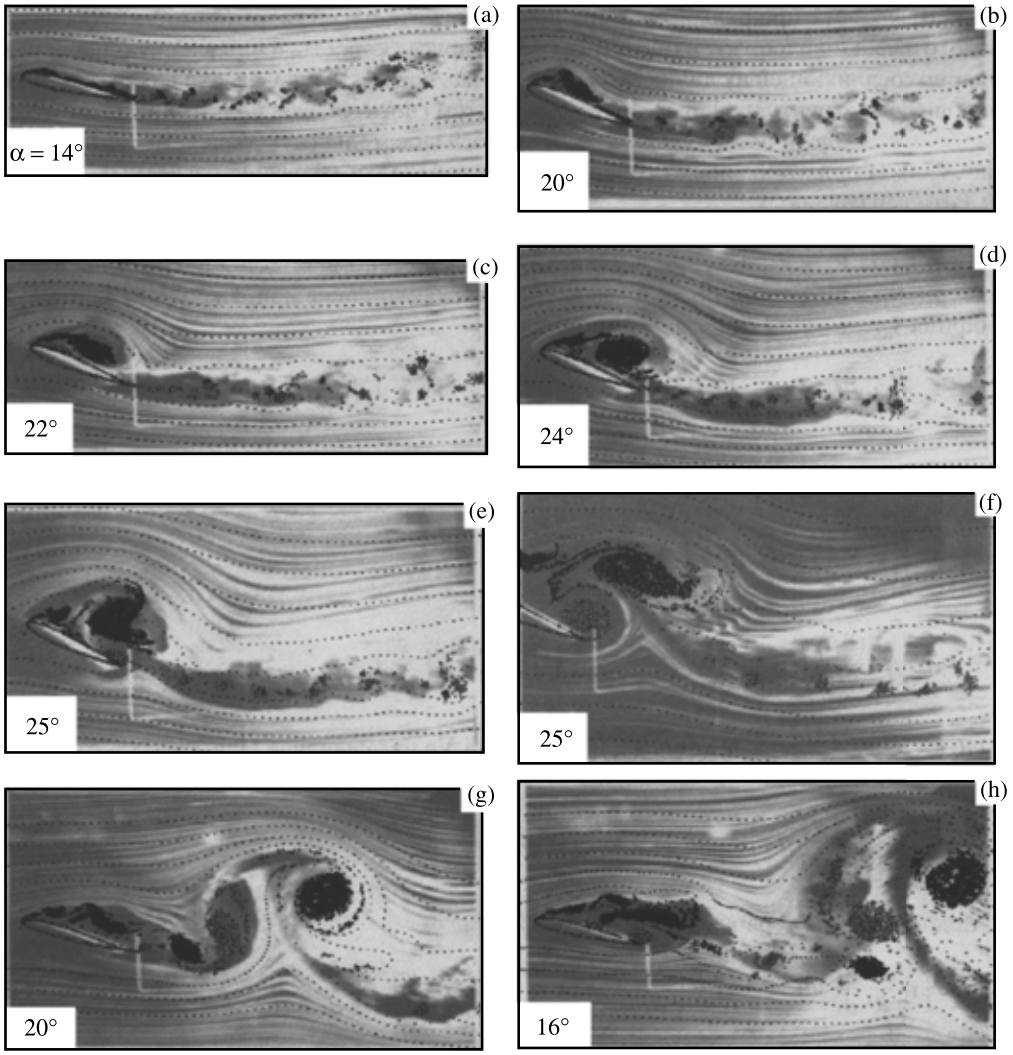

Fig. 2. Comparison of the calculated and experimental flowfields for the oscillating NACA-0012 airfoil at $\alpha_0 = 15^\circ$, $\alpha_1 = 10^\circ$, $h = 0.25$, $k = 0.2$, and $\mathrm{Re} = 4.4 \times 10^4$ in the stages of increase (a)–(e) and decrease (f)–(h) in the angle of attack α.

contributions decay exponentially with the distance to the observation point, both the contribution of a distant domain and the error in calculating it turn out to be unimportant.

The viscous vortex domain method was tested against certain model problems of unsteady separated flow past bodies at different Reynolds numbers [8]; the results obtained were compared with the available experimental data and the numerical results of other authors obtained by finite-difference methods.

3. CALCULATED RESULTS FOR THE FLOWFIELD

The flow over an oscillating wing was calculated with reference to the NACA-0012 airfoil at $\alpha_0 = 15^\circ$, $\alpha_1 = 10^\circ$, $h = 0.25$, $k = 0.2$, and $\mathrm{Re} = 4.4 \times 10^4$. These parameter values were chosen for comparison with the experimental data [1], where the flow patterns in different wing oscillation stages were obtained using smoke visualization. In the calculations, the number of division points on the contour was 247, while the time step was equal to 0.004. After just two oscillation periods, a quasi-periodic regime of flow past the airfoil was attained. The comparison with experiment was carried out for the third oscillation period; at this point, the number of vortex domains amounted to 6 to 8 thousand.

In Fig. 2 the experimental smoke-visualization pictures [1] are matched with the calculated positions of

the vortex domains; the light and dark circles correspond to domains with positive and negative circulations, respectively. In the same figure, the broken curves represent the calculated positions of the passive admixture "emitted" from points ahead of the airfoil. In Fig. 2a to 2e, (the stage of increase of the angle of attack) the process of large vortex formation on the leeward side of the airfoil is visible. The vortex is formed chiefly by negative-circulation, or clockwise, domains born on the leading edge. When these domains are displaced downstream, their circulation turns out to be excessive for ensuring the no-slip condition on the downstream portion of the contour; as a consequence, a positive vorticity is formed there, together with a flow between the two vortex formations directed from the trailing to the leading edge. This flow decelerates the displacement of the negative-circulation vortex and this circulation accumulates, since on the leading edge vortex generation continues. On the other hand, the counterflow fills the separation zone with fluid (air) which gradually pushes the vortex downstream.

As the angle of attack reaches a maximum and begins to decrease (Fig. 2e and 2f), the negative circulation "excess" increases, thus accelerating the process of vortex displacement into the cocurrent flow. After the negative-circulation vortex has been carried away, the positive circulation formed below it also turns out to be excessive. It is subjected to a process which is similar but shorter, since the positive vortex is supplemented from the trailing edge. As a result, following a large negative vortex, a large positive vortex is shed from the airfoil (Fig. 2f). The two vortices of opposite sign induce in each other's vicinity a velocity directed perpendicular to the line connecting them (in this case, upward). The ascending vortices form a mushroom-shaped structure (Fig. 2h) which is then convected downstream. Then a series of smaller vortices is similarly shed from the airfoil (Fig. 2g). The figures demonstrate good qualitative agreement between the calculated and experimental data.

4. CALCULATION OF TIME-DEPENDENT HYDRODYNAMIC FORCES

Let us derive general expressions for the force $\mathbf{F}_p + \mathbf{F}_\tau$ acting on the body in a viscous flow in terms of the vortex field parameters

$$\mathbf{F}_p = \oint_C \mathbf{n} p\, dl, \qquad \mathbf{F}_\tau = \oint_C \boldsymbol{\tau}\, dl,$$

where p is the pressure and $\boldsymbol{\tau}$ is the tangential stress on the contour C of the airfoil S_a.

The pressure force $\mathbf{F}_p$ can be brought into the form:

$$\mathbf{F}_p = \oint_C \left(\mathbf{e}_z \times \frac{\partial \mathbf{r}}{\partial l}\right) p\, dl = \mathbf{e}_z \times \oint_C p \frac{\partial \mathbf{r}}{\partial l}\, dl$$
$$= \mathbf{e}_z \times \left(\oint_C \frac{\partial \mathbf{r} p}{\partial l}\, dl - \oint_C \mathbf{r} \frac{\partial p}{\partial l}\, dl\right) = -\mathbf{e}_z \times \oint_C \mathbf{r}\left(\frac{\partial \mathbf{r}}{\partial l} \nabla p\right) dl.$$

Substituting the expressions for the gradient ∇p from the Navier–Stokes equation in form (1.3) in the above equation yields

$$\mathbf{F}_p = \mathbf{e}_z \times \oint_C \mathbf{r}\left(\frac{d\mathbf{V}}{dt}\, d\mathbf{r}\right) - \mathbf{e}_z \times \oint_C \mathbf{r}((\mathbf{V}_d \times \boldsymbol{\Omega})\, d\mathbf{r}). \tag{4.1}$$

We now transform the first term of Eq. (4.1) as follows:

$$\mathbf{e}_z \times \oint_C \mathbf{r}\left(\frac{d\mathbf{V}}{dt}\frac{\partial \mathbf{r}}{\partial l}\right) dl = -\oint_C \mathbf{r} \times \left(\frac{d\mathbf{V}}{dt} \times \left(\mathbf{e}_z \times \frac{\partial \mathbf{r}}{\partial l}\right)\right) dl = -\oint_C \mathbf{r} \times \left(\frac{d\mathbf{V}}{dt} \times \mathbf{n}\right) dl. \tag{4.2}$$

By virtue of the no-slip condition, the fluid velocity on the contour is equal to the velocity of the contour itself

$$\mathbf{V} = \mathbf{V}_0 + \boldsymbol{\omega} \times (\mathbf{r} - \mathbf{r}_0). \tag{4.3}$$

Therefore, its total time derivative coincides with the acceleration of points on the contour

$$\frac{d\mathbf{V}}{dt} = \dot{\mathbf{V}}_0 - \omega^2(\mathbf{r} - \mathbf{r}_0) + \dot{\boldsymbol{\omega}} \times (\mathbf{r} - \mathbf{r}_0). \tag{4.4}$$

Here, $\mathbf{V}_0$ and $\mathbf{r}_0$ are the velocity and radius-vector of the point about which the airfoil rotates and $\boldsymbol{\omega}$ is the angular velocity vector.

Substituting Eq. (4.4) in Eq. (4.2) and evaluating the integrals we obtain

$$\begin{aligned}
\mathbf{e}_z \times \oint_C \mathbf{r}\left(\frac{d\mathbf{V}}{dt}\frac{\partial \mathbf{r}}{\partial l}\right) dl &= -\oint_C \mathbf{r} \times ((\dot{\mathbf{V}}_0 - \omega^2(\mathbf{r} - \mathbf{r}_0) + \dot{\boldsymbol{\omega}} \times (\mathbf{r} - \mathbf{r}_0)) \times \mathbf{n})\, dl \\
&= -\int_{S_a} \mathbf{r} \times (\boldsymbol{\nabla} \times (\dot{\mathbf{V}}_0 - \omega^2(\mathbf{r} - \mathbf{r}_0) + \dot{\boldsymbol{\omega}} \times (\mathbf{r} - \mathbf{r}_0)))\, ds \\
&\quad - \int_{S_a} ((\dot{\mathbf{V}}_0 - \omega^2(\mathbf{r} - \mathbf{r}_0) + \dot{\boldsymbol{\omega}} \times (\mathbf{r} - \mathbf{r}_0)) \times \boldsymbol{\nabla}) \times \mathbf{r}\, ds \\
&= -\mathbf{r}_m \times 2\dot{\boldsymbol{\omega}} S_a + \dot{\mathbf{V}}_0 S_a - \omega^2(\mathbf{r} - \mathbf{r}_0) S_a + \dot{\boldsymbol{\omega}} \times (\mathbf{r} - \mathbf{r}_0) S_a,
\end{aligned} \tag{4.5}$$

where $\mathbf{r}_m$ is the radius-vector of the center of the region S_a.

The second term of Eq. (4.1) can be written in the form:

$$\begin{aligned}
-\mathbf{e}_z \times \oint_C \mathbf{r}((\mathbf{V}_d \times \boldsymbol{\Omega})\, d\mathbf{r}) &= \oint_C \mathbf{r} \times \mathbf{e}_z \left((\mathbf{V}_d \times \boldsymbol{\Omega}) \frac{\partial \mathbf{r}}{\partial l}\right) dl \\
&= \oint_C \mathbf{r} \times \left((\mathbf{V}_d \times \boldsymbol{\Omega}) \times \left(\mathbf{e}_z \times \frac{\partial \mathbf{r}}{\partial l}\right)\right) dl = \oint_C \mathbf{r} \times ((\mathbf{V}_d \times \boldsymbol{\Omega}) \times \mathbf{n})\, dl = \oint_C \mathbf{r} \times \boldsymbol{\Omega}(\mathbf{V}_d \mathbf{n})\, dl.
\end{aligned} \tag{4.6}$$

The quantity $\boldsymbol{\Omega}(\mathbf{V}_d \mathbf{n})\, dl$ is the vorticity flux $\mathbf{J}\, dl$ from the body surface to the fluid taken with the opposite sign. Substituting Eqs. (4.5) and (4.6) in Eq. (4.1), we obtain the final expression for the pressure force

$$\mathbf{F}_p = \dot{\mathbf{V}}_0 S_a - \omega^2(\mathbf{r}_m - \mathbf{r}_0) S_a + \dot{\boldsymbol{\omega}} \times (3\mathbf{r}_m - \mathbf{r}_0) S_a - \oint_C \mathbf{r} \times \mathbf{J}\, dl.$$

In the numerical simulation the flux $\mathbf{J}\, dl$ is taken as the circulation $\Gamma^{(g)}$ of the vortices formed near the control element dl in time Δt (the circulations of the vortices eliminated because of their penetration inside the contour are included in J with the opposite sign) divided by Δt. Correspondingly, in the discrete representation the contour integral is determined by the sum

$$\oint_C \mathbf{r} \times \mathbf{J}\, dl \approx \sum_k \mathbf{r}_k \times \frac{\Gamma_k^{(g)}}{\Delta t}.$$

In a viscous incompressible flow the stress tensor takes the form [7]:

$$\mathbf{P} = \begin{pmatrix} -p + 2\dfrac{1}{\mathrm{Re}}\dfrac{\partial V_x}{\partial x} & \dfrac{1}{\mathrm{Re}}\left(\dfrac{\partial V_x}{\partial y} + \dfrac{\partial V_y}{\partial x}\right) \\ \dfrac{1}{\mathrm{Re}}\left(\dfrac{\partial V_x}{\partial y} + \dfrac{\partial V_y}{\partial x}\right) & -p + 2\dfrac{1}{\mathrm{Re}}\dfrac{\partial V_y}{\partial y} \end{pmatrix}.$$

The viscous stress $\boldsymbol{\tau}$ acting on the body over an area $\Delta\mathbf{s} = \mathbf{n}\Delta s$ is expressed by the formula

$$\boldsymbol{\tau} = -\frac{1}{\mathrm{Re}}\begin{pmatrix} 2\dfrac{\partial V_x}{\partial x} & \left(\dfrac{\partial V_x}{\partial y} + \dfrac{\partial V_y}{\partial x}\right) \\ \left(\dfrac{\partial V_x}{\partial y} + \dfrac{\partial V_y}{\partial x}\right) & 2\dfrac{\partial V_y}{\partial y} \end{pmatrix}\begin{pmatrix} n_x \\ n_y \end{pmatrix}$$

$$= -\frac{2(\boldsymbol{\nabla}\mathbf{V})}{\mathrm{Re}}\begin{pmatrix} 1 & 0 \\ 0 & 1 \end{pmatrix}\begin{pmatrix} n_x \\ n_y \end{pmatrix} + \frac{2}{\mathrm{Re}}\begin{pmatrix} \dfrac{\partial V_y}{\partial y} & -\dfrac{\partial V_y}{\partial x} \\ -\dfrac{\partial V_x}{\partial x} & \dfrac{\partial V_x}{\partial x} \end{pmatrix}\begin{pmatrix} n_x \\ n_y \end{pmatrix}$$

$$-\frac{1}{\mathrm{Re}}\begin{pmatrix} 0 & \left(\dfrac{\partial V_x}{\partial y} - \dfrac{\partial V_y}{\partial x}\right) \\ \left(\dfrac{\partial V_y}{\partial x} - \dfrac{\partial V_x}{\partial y}\right) & 0 \end{pmatrix}\begin{pmatrix} n_x \\ n_y \end{pmatrix}$$

$$= -\frac{1}{\mathrm{Re}}(2\mathbf{n}(\boldsymbol{\nabla}\mathbf{V}) - 2(\mathbf{n}\times\boldsymbol{\nabla})\times\mathbf{V} + \mathbf{n}\times(\boldsymbol{\nabla}\times\mathbf{V})).$$

Since in an incompressible flow $\nabla\mathbf{V} = 0$, we obtain

$$\boldsymbol{\tau} = -2\frac{1}{\mathrm{Re}}(\mathbf{n}\times\boldsymbol{\nabla})\times\mathbf{V} + \frac{1}{\mathrm{Re}}\mathbf{n}\times\boldsymbol{\Omega}. \tag{4.7}$$

The operator $\mathbf{n}\times\boldsymbol{\nabla}$ does not contain derivatives normal to the airfoil contour C, while, under the no-slip condition, the fluid velocity is equal to the contour velocity determined by formula (4.3). Therefore, in Eq. (4.7) we have

$$(\mathbf{n}\times\boldsymbol{\nabla})\times\mathbf{V} = (\mathbf{n}\boldsymbol{\nabla})\mathbf{V} + \mathbf{n}\times(\boldsymbol{\nabla}\times\mathbf{V}) - \mathbf{n}(\boldsymbol{\nabla}\mathbf{V}) = (\mathbf{n}\boldsymbol{\nabla})(\boldsymbol{\omega}\times\mathbf{r}) + \mathbf{n}\times 2\boldsymbol{\omega}$$
$$= (\boldsymbol{\omega}\times(\mathbf{n}\boldsymbol{\nabla})\mathbf{r}) + \mathbf{n}\times 2\boldsymbol{\omega} = (\boldsymbol{\omega}\times\mathbf{n}) + \mathbf{n}\times 2\boldsymbol{\omega} = \mathbf{n}\times\boldsymbol{\omega}.$$

Substituting this expression in Eq. (4.7), for the tangential stress on the rigid contour we obtain

$$\boldsymbol{\tau} = \frac{1}{\mathrm{Re}}(\mathbf{n}\times\boldsymbol{\Omega} - 2\mathbf{n}\times\boldsymbol{\omega}).$$

The friction force $\mathbf{F}_\tau$ acting on the contour as a whole is as follows:

$$\mathbf{F}_\tau = \oint_C \boldsymbol{\tau}\, dl = \frac{1}{\mathrm{Re}}\oint_C \mathbf{n}\times\boldsymbol{\Omega}\, dl \approx \frac{1}{\mathrm{Re}}\sum_k \mathbf{n}_k\times\boldsymbol{\Omega}_k d_k.$$

Since, according to Eq. (2.2), we have

$$\boldsymbol{\Omega}_k \approx \frac{1}{s_k}\sum_i \boldsymbol{\Gamma}_i \exp\left(-\frac{r_{ik}}{\varepsilon_k}\right)$$

using Eq. (2.6) and the condition of the equality of ε_i and ε_k we can write $\mathbf{F}_\tau$ in the form:

$$\mathbf{F}_\tau = \sum_k\sum_i \frac{1}{s_k}\mathbf{w}_{ik}\times\boldsymbol{\Gamma}_i s_i.$$

In Fig. 3 the angle-of-attack dependence of the wing lift coefficient in the process of unsteady motion obtained in this study is compared with the experimental data [1] and [9]. In [1] the lift was indirectly

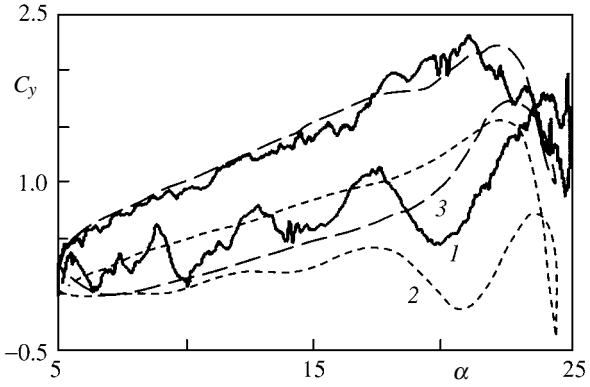

Fig. 3. Lift coefficient: (*1*) and (*2*) calculation and experiment [1] for $k = 0.16$ and $\mathrm{Re} = 4.4 \times 10^4$ and (*3*) experiment [9] for $k = 0.153$ and $\mathrm{Re} = 4.8 \times 10^4$.

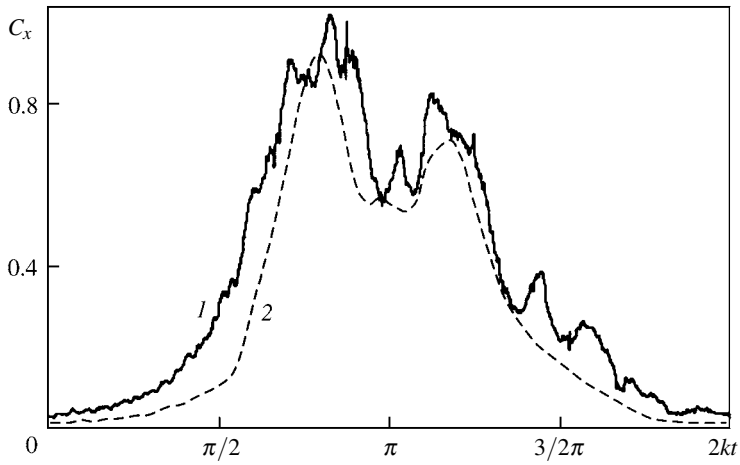

Fig. 4. Drag coefficient: (*1*) calculation and (*2*) experiment [9].

calculated by means of approximate formulas on the basis of measurements of the velocity distribution averaged over several oscillation periods in a section perpendicular to the oncoming flow at a distance of $0.3L$ from the airfoil (Fig. 1). From these measurements, the authors of [1] calculated the vorticity flux from the airfoil and then, using the data thus obtained, the lift variation by means of the Joukowski formula. The accuracy of the results thus obtained is poor, which is acknowledged by the authors of [1].

In [9] the pressure was directly measured at a number of points on the airfoil; then the lift coefficient was calculated by integration. Clearly, the calculated data are in good agreement with experiment [9]. The results obtained in [1] are qualitatively the same but lie lower.

In all three cases, hysteresis takes place. Near the point of maximum angle of attack, a sharp decrease in the lift is observable at the moment of negative-circulation vortex shedding; then it increases rapidly due to shedding of a positive vortex. Furthermore, the results of both this study and [1] indicate the oscillation of the lift variation about a lower value than in the case of increase in α. In both cases, the oscillation amplitudes and periods are in agreement.

The calculated time dependences of the drag coefficient obtained in this study and [9] are compared in Fig. 4 for the same values of the parameters as in Fig. 3. Clearly, the results are in good qualitative and satisfactory quantitative agreement (it should be borne in mind that the data were obtained by averaging over many periods).

Summary. Using the viscous vortex domain method for modeling the two-dimensional flow past an oscillating airfoil makes it possible adequately to reproduce the time-dependent processes of large vortex formation and shedding which lead to lift hysteresis. The numerical calculation of the passive admixture

tracks yields flowfields which almost coincide with the experimental flow patterns obtained by smoke visualization. Formulas for calculating the unsteady stresses on the surface of a body in a viscous flow are derived in terms of the vorticity distribution in the ambient space. The calculated lift coefficients are in agreement with the experimental data. The computational technique developed in the study makes it possible to analyze the hydrodynamic mechanisms of generation of time-dependent loads on an oscillating wing.

The study was carried out with the support of the Russian Foundation for Basic Research (projects Nos. 04-01-00554 and 06-08-01217) and the Program Nsh-8597.2006.1.

REFERENCES

1. J. Panda and K.B.M.Q. Zaman, "Experimental Investigation of the Flow Field of an Oscillating Airfoil and Estimation of Lift from Wake Surveys," J. Fluid Mech. **265**, 65–95 (1994).
2. S.V. Guvernyuk, "New possibilities of computational vortex methods for modeling time-dependent two-dimensional viscous flows," in: *Proceedings of the International Conference "Nonlinear Problems of Hydrodynamic Stability Theory and Turbulence"* [in Russian], Moscow Univ. Press, Moscow (2004), 97–102.
3. G.Ya. Dynnikova, "Lagrangian approach to the solution of time-dependent Navier–Stokes equations," Dokl. Ross. Akad. Nauk **399**, 42–46 (2004).
4. Y. Ogami and T. Akamatsu, "Viscous Flow Simulation Using the Discrete Vortex Model. The Diffusion Velocity Method," J. Computers Fluids **19**, 433–441 (1991).
5. G.Ya. Dynnikova, "Vortex motion in two-dimensional viscous fluid flows," Fluid Dynamics **38**, 670 (2003).
6. G.K. Batchelor, *Introduction to Fluid Dynamics* (Cambridge Univ. Press., Cambridge, 1967).
7. L.G. Loitsyanskii, *Mechanics of Liquids and Gases*, Pergamon Press, Oxford (1966).
8. P.R. Andronov, A.I. Gircha, S.V. Guvernyuk, and G.Ya. Dynnikova, "Certain results of testing the viscous vortex domain method for solving problems of incompressible fluid dynamics," in: *Proceedings of the 5th International Workshop "Models and Methods in Aerodynamics"* [in Russian], Moscow (2005), p. 13.
9. K.W. McAlister, S.L. Pucci, W.L. McCroskey, and L.W. Carr, "An experimental study of dynamic stall in advanced airfoil sections. Vol. 2. Pressure and force data," NASA TM 84245 (1982).